

## **Geophysical Interpretation of Geological Features Constraining Bitumen Deposit In Agbabu, Southwestern Nigeria**

<sup>1</sup>Ogungbemi, Oluwaseun S., <sup>2</sup>Ogunyemi, Adebayo T., <sup>3</sup>Obaniwa, Mimololuwa M.

<sup>1,2,3</sup>*Department of Chemical and Petroleum Engineering,  
AfeBabalola University, Ado-Ekiti, Ekiti State, Nigeria  
Corresponding Author: Ogungbemi*

---

**Abstract:** *Litho-structural settings of Agbabu was interpreted using aero-magnetic and aero-radiometric data with the aim of delineating geological features constraining bitumen deposit in that area. Geological features (transition zone, basement ridges and depression) constraining bitumen deposit exhibit relatively low (-159.3 – 17.1 nT) total magnetic intensity (TMI) and high analytic signal (A.S) amplitude (0.064 – 0.195) as against other regions where high TMI values (22.3 – 91.0 nT) correspond to low AS values. The low amplitude (-1.4 – 0.1) from the tilt derivative (TDR) filter also confirm the concealed basement depression hosting bitumen deposit. The 3D-Euler filter helps to locate the sources of magnetic anomalies as deeper within the sedimentary terrain (423.6 – 1012 m) and shallower (144.3 – 315.4 m) within the basement. The depth to basement (764.1 and 1012 m) around Agbabu area, partly account for the large volume of bitumen deposit in this area. The interpretations of radiometric datasets revealed the spatial variation of potassium (K), thorium (Th) and uranium (U) radioelement concentrations as high (0.6 – 25%), (9.2 – 28.0 ppm) and (2.4 – 5.1 ppm) respectively within the basement complex, but low (0.0 – 0.5%), (1.8 – 8.5 ppm) and (0.3 – 2.2 ppm) respectively within the sedimentary terrain. The ternary image shows very low radiometric intensity at areas containing the bitumen deposit and moderately high around lithological boundaries and concealed linear features. This study offers important geologic information that will make estimation and exploitation of the bitumen in Agbabu less cumbersome.*

**Keywords:** *Geological, Features, Constraining, Bitumen, Agbabu*

---

Date of Submission: 03-08-2019

Date of acceptance: 19-08-2019

---

### **I. Introduction**

There is significant diversification in Nigeria's economy before the discovery of oil and gas which currently accounts for about 80% of the country's revenue. Hydrocarbon potentials of the prolific oil-rich Niger Delta will in the near future become depleted or exhausted due to continuous exploitation and over dependence as major source of revenue. Asphalt-impregnated sandstones otherwise referred to as oil sands (tar sands) and active oil-seepages occur in south-western Nigeria within the marginal pull-apart or margin-sag Dahomey (Benin) basin. The oil sands outcrop in an E-W belt, approximately 140 km long and 4 – 6 km wide, extending from Edo, Ondo and Ogun State in southwest Nigeria (Adegoke and Omatsola, 1981). Therefore, attention must be shifted to other potential source of revenue such as the bitumen exploitation in Nigeria. In this study, the occurrence and lithostructural settings of bitumen in Agbabu was investigated due to its economic importance as an alternative source of energy and income (Obiora et al., 2015). Airborne magnetic and radiometric datasets have been used to interpret the geological structures and potential mineralization zones by Wemegahet al., (2015). Airborne magnetic and radiometric surveys have been used extensively in the mineral exploration industry to delineate metallic and non-metallic deposits in most parts of the world (Keating, 1995).

### **Geology and Description of the Study Area:**

Agbabu (the study area) is located within the geographical grids of latitude 6° 35' 16.3"N and 6° 40' 13.9" N and longitude 4° 49' 29.0" E and 5° 00' 20.7"E in Odigbo local government area of Ondo State. It falls within the sedimentary terrain in the Dahomey basin of south-western, Nigeria. The Dahomey basin is an Atlantic margin basin containing Mesozoic-Cenozoic sedimentary succession reaching a thickness of over 3,000m. It extends from south-eastern Ghana to the western flank of the Niger Delta. Its stratigraphy is classified by various authors into Abeokuta Group, Imo Group, Oshosun Formation, Ilaro Formation and Coastal Plain sands and Alluvium (Jones and Hockey, 1964, Adegoke and Omatsola, 1981). The Agbabu area is underlain by the sediments of the Imo Group.

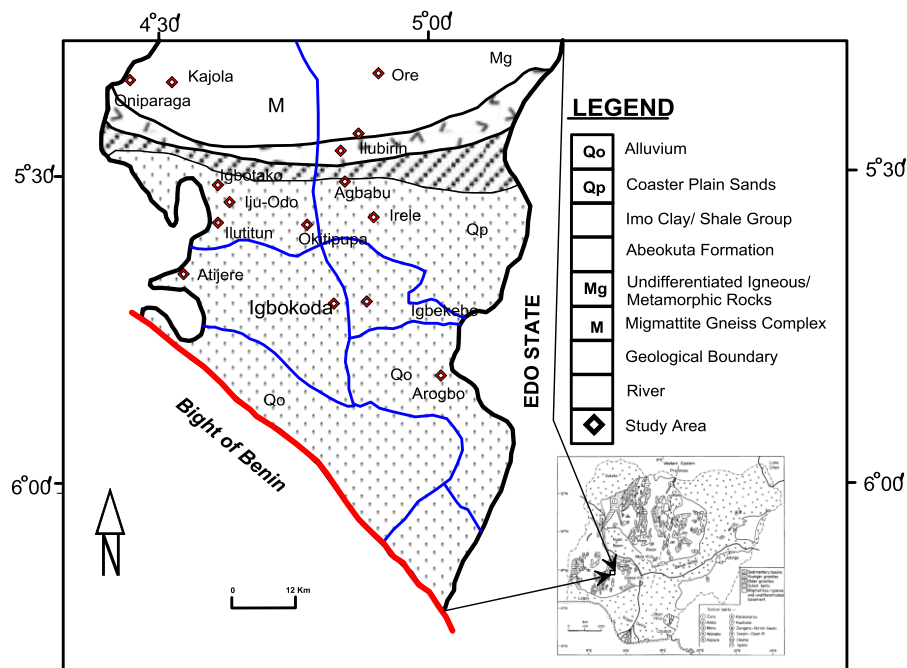


Figure1: Geological Map of southern part of Ondo State showing the Study Area (After PTF, 1997).

### Aeromagnetic Data

Even though the magnetic survey has been used extensively in mapping of mineral deposits for decades, modern advancement in acquiring magnetic data, processing and interpretations have amplified the significance of magnetic methods; predominantly the high resolution aeromagnetic survey (Clark, 1997).

The original data in the GDB (geodata base) format, after having been projected into Longitude and Latitude Coordinate System (using Geosoft software), the geographical coordinates of the study area (also in longitude and latitude) was superimposed to extract the database for this project. The minimum curvature technique was applied using the grid and image tool in gridding the extracted database for both the radiometric and magnetic data. The magmap tool offering a number of utilities was implemented to assist magnetic-anomaly grid (observed magnetic field less the Definitive International Geomagnetic Reference Field) to be calculated for the right time of year and altitude of the aircraft during survey and apply the following filters

### Magnetic Data Processing

A range of filters were applied to the aeromagnetic data to enhance anomalies of selected geologic features thereby transforming it to other grids in readiness for interpretation. The reduction to pole transform was applied to provide a symmetrical anomaly over a vertically dipping, non-remanent body. Derivative filters which include analytic signal (AS), tilt derivative (TDR) and 3D-euler deconvolution (ED), were applied to aeromagnetic data to sharpen edges of anomalies from high frequency, low amplitude local features (which were overshadowed by responses from regional features) at the same time enhancing low frequency, large amplitude features (Geosoft Inc., 1995, Milligan and Gunn, 1997). The analytic signal grid is computed from the existing derivative grids. It is the square root of the sum of the squares of the derivative in the x, y, and z directions.

$$\text{Analytic Signal (AS)} = \sqrt{\partial x * \partial x + \partial y * \partial y + \partial z * \partial z}.$$

The Tilt derivative (TDR) filter, (a very good edge detection filter) was applied to bring out short wavelength and reveals the presence of magnetic lineaments. Tilt derivative is calculated using this relation below:

$$\text{TDR} = \tan^{-1} \left( \frac{\text{VDR}}{\text{THDR}} \right)$$

Where VDR and THDR are the first vertical and horizontal derivatives of the total magnetic field intensity (TMI) respectively

### Airborne Radiometric Data

Airborne radiometric data helped to map lithology of the area. Most often, a better relationship is recognized in the radiometric data around rocks that are weathered and unweathered. These data when correlated with that of electromagnetic, magnetic and geochemical are usually helpful in the explorations of mineral deposits (Gunn et al., 1997; Shives et al., 2000).

This is one of the most rapid techniques for soil chemistry surveying of the uranium, thorium and potassium. This part explains some enhancing techniques of the radiometric data which include ternary, Ratio, Potassium, Thorium and Uranium maps for the study area. The purpose of enhancing the data is to identify and interpret signatures related with the source rocks for potential mineralization.

### **Radiometric Data Processing**

Uranium (U), Thorium (Th) and Potassium (K) are the three commonest, naturally occurring radionuclides on Earth. In order to delineate geological units and interpret radiometric signatures associated with different lithology, enhanced images such as ternary image, potassium (K), thorium (Th) and uranium (U) concentration maps were produced (Ostrovskiy, 1975). The ternary image in red-green-blue (RGB) colour model was created using Geosoft software for which potassium, thorium and uranium were assigned to red, green and blue respectively. Histogram equalization was applied to give the best colour variation by enhancing the contrast of the individual components of K, Th and U before combining into a single image.

## **II. Results and Discussion of Results**

### **Aeromagnetic Data Interpretation**

The original Total Magnetic Intensity (TMI) grid (Fig. 2) was processed and filtered to enhanced weak, small-sized magnetic anomalies from shallow sources and at the same time enhancing low-amplitude, long-wavelength magnetic anomalies from deeper sources. The total magnetic intensity map is characterized by the presence of high and low magnetic intensity. Magnetic anomalies are generally high (22.3 to 91.0 nT) around the southern, south-western, western, eastern, north-western and north-eastern regions, while the low intensity anomalies (-159.3 – 17.1 nT) occur mainly around the central and south-eastern region, where bitumen deposit occur. Aeromagnetic maps reveal major structures such as magnetic dykes, ridges and depressions, linear to curvilinear features and the overall basement characteristics.

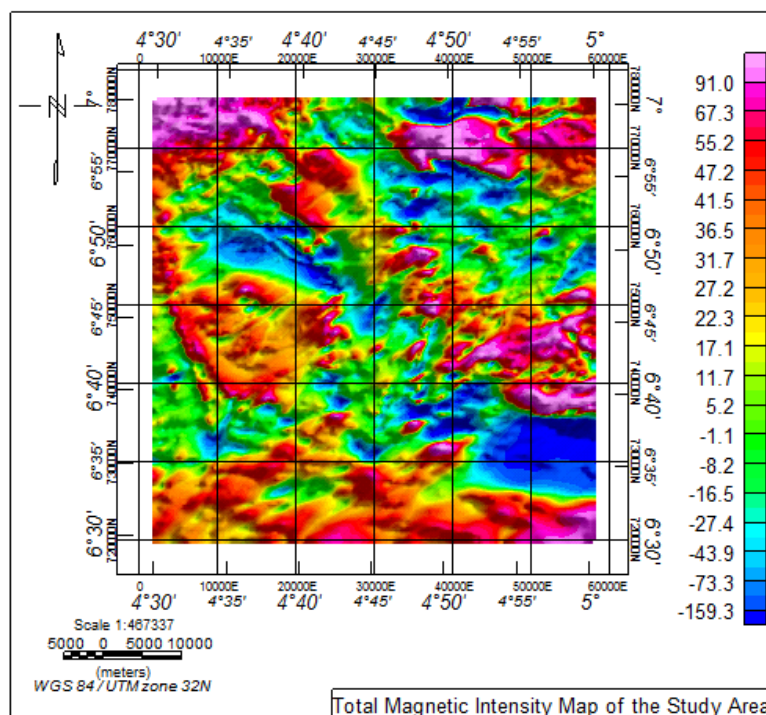


**Figure 2:** Total Magnetic Intensity Map of the Study Area.

Analytic signal filter which was applied to the TMI data helps to clearly define the edge of magnetic anomaly sources such as lithological contacts and other concealed geological features within the study area (Debeglia and Corpel, 1997, Oruc and Selim, 2011). The variation in the amplitudes of the analytic signal map (Fig. 3) shows the spatial distributions of causative magnetic source bodies within the study area. High amplitudes (0.064 – 0.195) are recorded around the northern, eastern, central and south-eastern part of the study area, while the remaining part exhibit low (- 0.086 – 0.054) response.

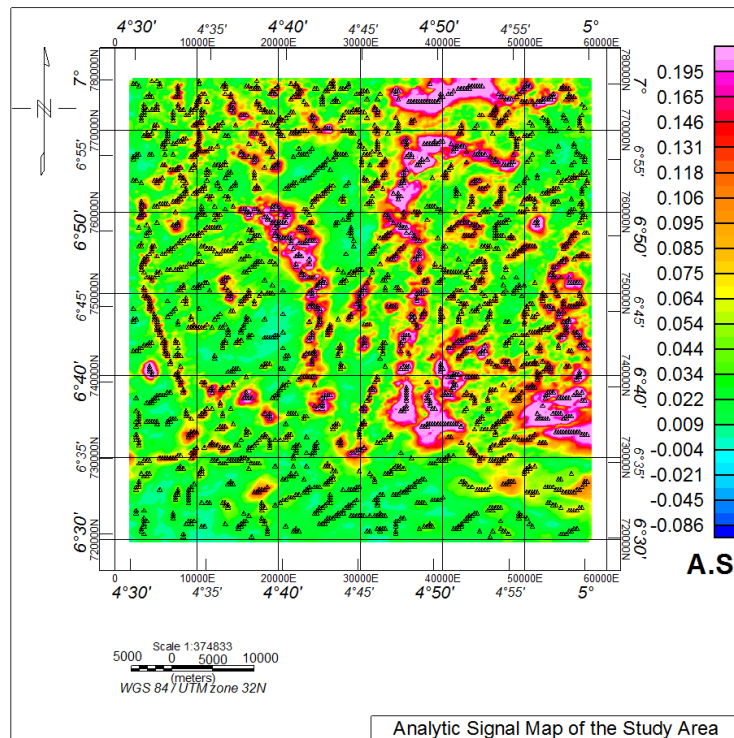


Figure 3: Analytic Signal magnetic map

The structures which give rise to high amplitude in the analytic signal map (Fig. 3) are identified with low magnetic anomalies in the TDR map (Fig. 4). Tilt angle derivative filter locates the edges of formations, using the theory that the zero contours are at the edges of the formation (Salem et al., 2007). The TDR shows the presence of large concealed structure suspected to be basement depression which host bitumen deposit where the response is low (-1.4 – 0.1).

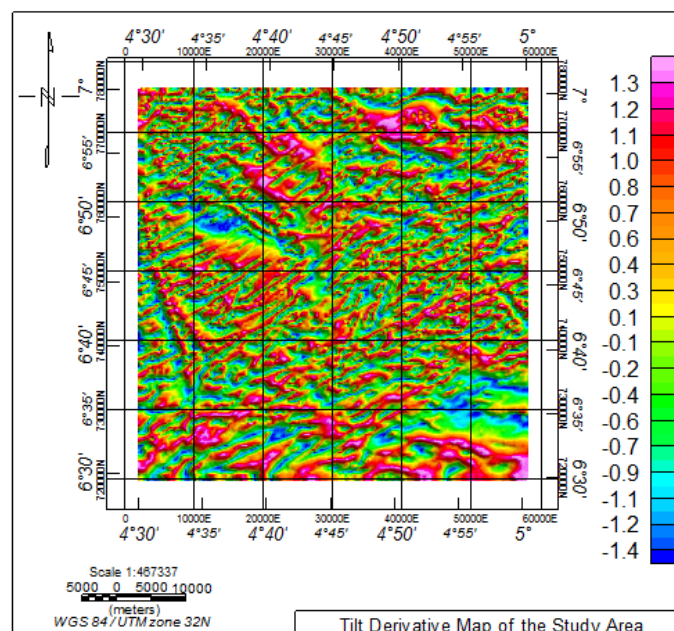
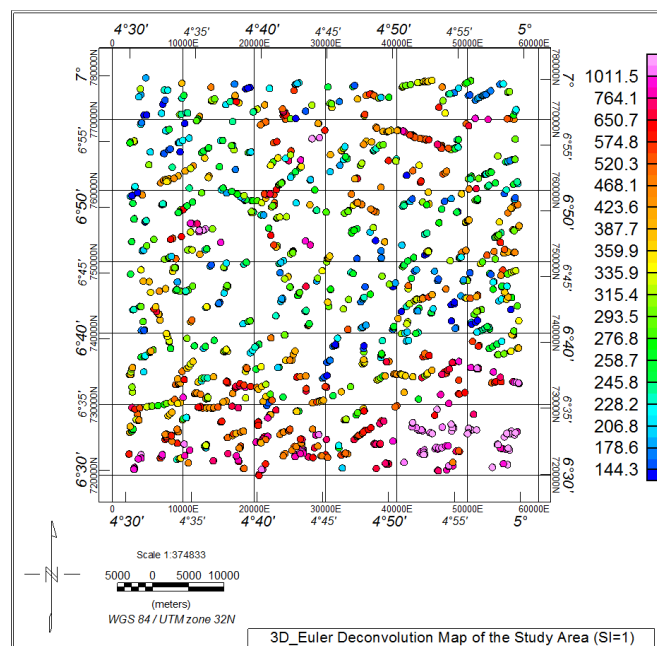


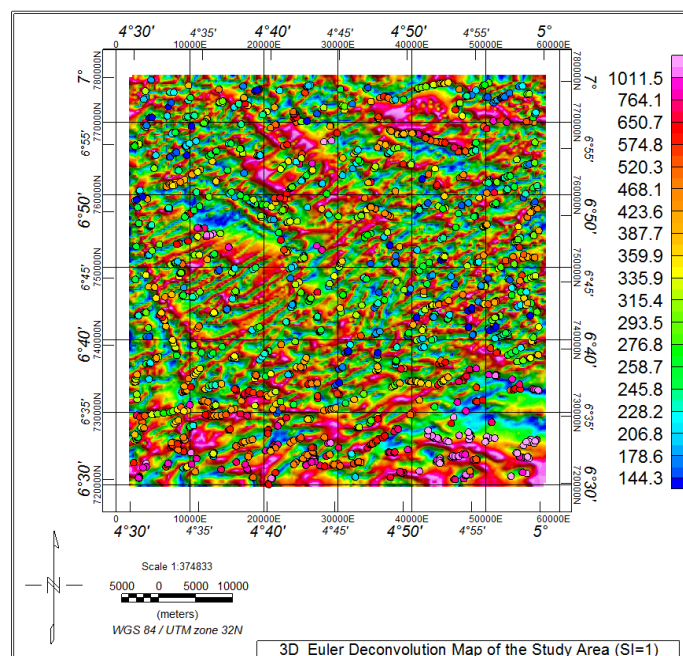
Figure 4: Tilt Derivative Map of the Study Area

Euler deconvolution (Reid et al., 1990) is an automatic technique used for locating the source of potential field based on both their amplitudes and gradients. It enhances both weak and strong magnetic anomalies associated with geological structures of the area. The solutions from the Euler deconvolution maps are generally located on the maximum peak of the analytic signal solutions. The peaks of the anomalous bodies are located with a cross (+) symbol and were further enhanced in the 3D-Euler deconvolution map to reveals the

locations and depths to source of magnetic anomalies (which ranges from 144 – 1,012 m) within this study area. The solutions (in circles) were produced by selecting structural index of 1.0 for the map. The depth to top of magnetic anomaly within the metasediment (where Agbabu is located) ranges between 423.6 – 1,011.5 m but shallower (144.3 – 315.4) within the Basement Complex. The depth to basement within Agbabu area (764.1 – 1,011.5 m) is more than the surrounding area. This partly account for the large volume of bitumen deposit in this area (Fig. 5a). In figure 5b, the Euler deconvolution solution was superimposed on the TDR map to visualize their degree of correlation. There is high level of correlation, as most of the Euler solutions fall within areas delineated as having low magnetic response. These are areas suspected to have high potential for deposits of minerals such as bitumen.



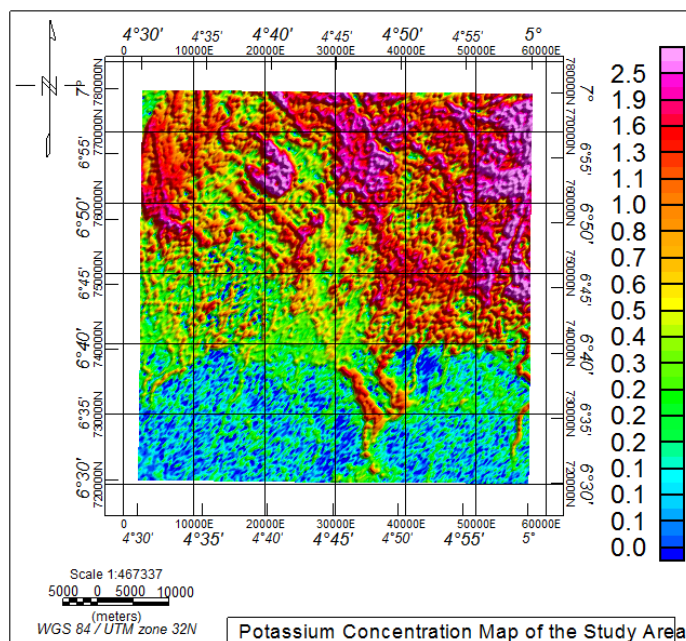
**Figure 5a:** 3D-Euler Deconvolution Map of the Study Area.



**Figure 5b:** 3D\_Euler and Tilt Derivative Map.

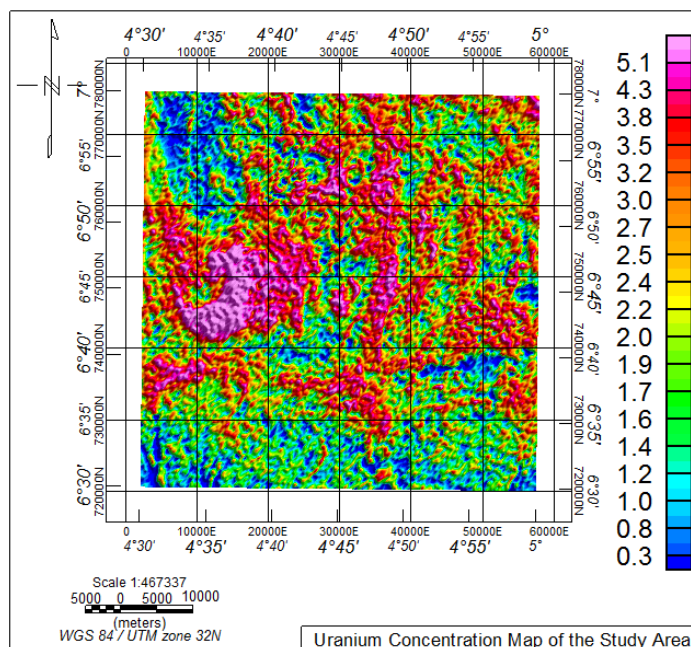
The analysis of radiometric survey data revealed various potassium (K), uranium (U) and thorium (Th) anomalies. Radiations of potassium basically emanates from potassium feldspar, predominantly micas which include muscovite and biotite (Boadiet al., 2013). Figure6 shows very high (0.6 – 2.5%) K-concentrations

within the Basement Complex, but relatively low (0.0 – 0.5%) within the sedimentary terrain which host the bitumen deposit.



**Figure 6:** Potassium (K) Concentration Map of the Study Area.

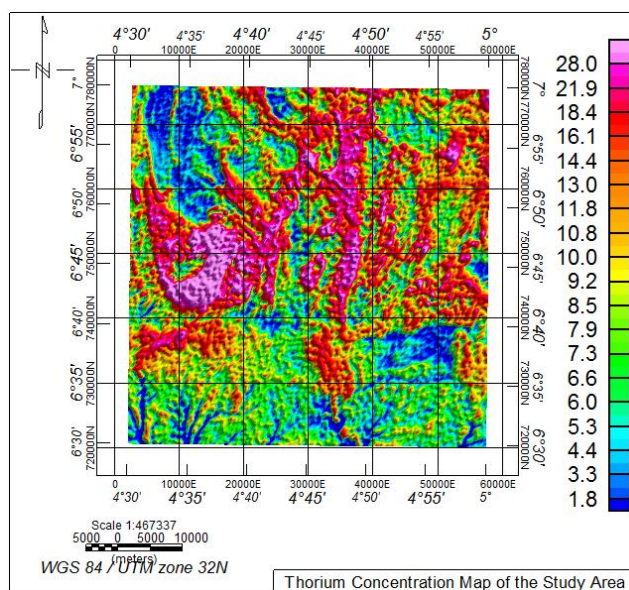
Thorium concentration anomalies map (Fig. 7), helped to delineate the boundaries of the basement and the sedimentary terrains. The north, northwest and northeast regions (which fall within the basement regions) of the study area produced relatively higher thorium concentrations (9.2 – 28.0 ppm). The sedimentary basin which is the south, southwest and southeast regions produced low intensities of immobile and mobile Thorium (Silva et al., 2003). The low concentration (1.8 – 8.5 ppm) within the sedimentary region implies great depth to basement rocks, hence there is a high potential of bitumen deposit in that area.



**Figure 7:** Thorium (Th) Concentration Map of the Radiometric Data

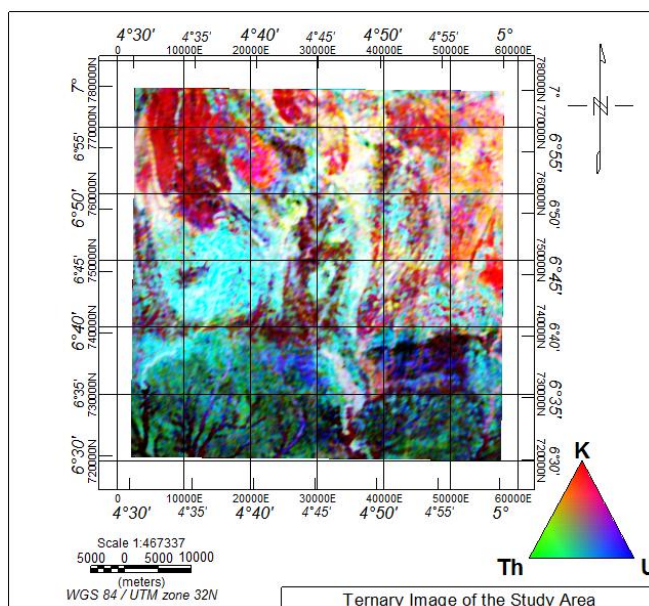
The Uranium concentration map (Fig 8) also emphasis the geological features shown in the Thorium map. The map shows the boundaries of the basement and the sedimentary basins. The north, northwest and northeast regions of the study area produced the higher uranium concentrations (2.4 – 5.1 ppm) and are related

partly with the basement rocks within that area. The sedimentary terrain which is the south, southwest and southeast regions produced low concentration of uranium (0.3 – 2.2 ppm) (Silva et al., 2003). From the map, it is evident that the southeast region has a very low intensity of uranium which also confirmed the deeper basement rock around the regions suspected to contain the bitumen deposit.



**Figure 8:** Uranium (U) Concentration Map of the Radiometric Data

The ternary image is a composite image produced from the concentrations of these gamma radiations (Fig. 9). Ternary images from radiometric data are an excellent tool for mapping and delineating lithological boundaries in an area (Silva et al., 2003). Variation of radioelement signature on the ternary map corresponds to changes in geological formation. Magnetite and quartz-rich rocks appear darker than the surrounding rocks, indicating lower concentrations in K, U, and Th. The whitish areas in the ternary image indicate high concentration of potassium, thorium and uranium resulting from felsic volcanic rocks. The yellowish region indicates areas with high count of potassium and thorium but low uranium count, the magenta colour shows areas with high potassium and uranium count but weak thorium count. The dark/light areas which coincides with magnetic anomalies (fractures, rock boundaries etc.) is attributed to some geologic processes such as weathering, alteration and shearing of rocks within these areas. The area containing bitumen deposit on this map appeared dark due to two main reasons. The first is that, the area falls within the sedimentary terrain, which is noted to have little or no amount of radioelements. Secondly, bitumen which has the highest percentage by volume of materials within the rock matrix has low gamma ray response. Thus, the area appear dark on the map.



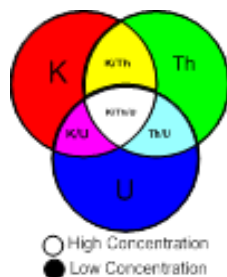


**Figure 9:** Ternary Image (K-Th-U/RGB) of the Study Area

Figure 10 reveals the aerial extent of bitumen within the study area. This area was marked out with red boundary line. It shows area or region of the study area containing large or significant quantities of bitumen deposit. The location of two old exploratory wells (Well 1 and Well 2) within the study area are denoted with blue square symbols. The map was also used to outline the sedimentary/basement boundary, which is indicated with yellow boundary lines. The basement region is towards the north above and sedimentary region towards the south below. The map also shows towns/villages as well as major road network within the area of study. Basement rock (ridge) which extends from the basement terrain to the sedimentary terrain (around the central region) partly constrained bitumen deposit from further migration to other adjoining parts.

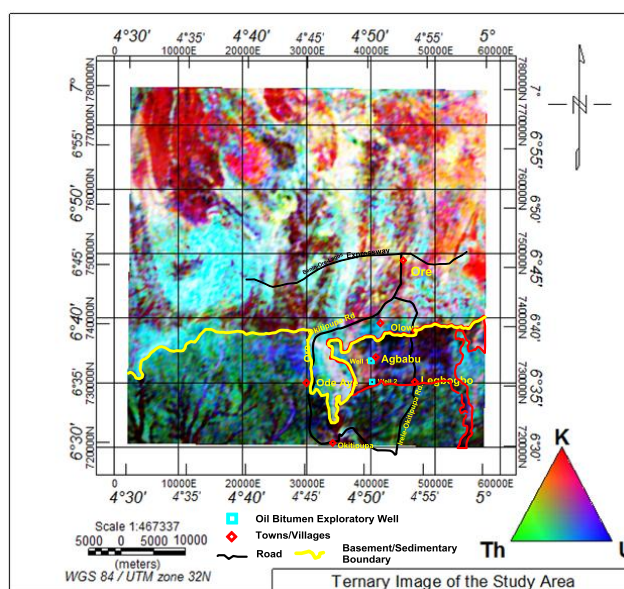


**Figure 10:** Ternary Map showing some Aerial Features

### III. Conclusions

Aeromagnetic and aeroradiometric datasets were successfully employed in delineating geological terrain of the study area (Agbabu). There are several methods, algorithms and software programs for quantitative interpretation of magnetic data so as to extract additional geological information from the magnetic data. Information about depth to source (which is also the depth to the magnetic basement) is contained in the geometry of the anomaly. Knowledge about depth to sources of magnetic anomalies and lithological boundaries give important clues about mineralisation zone potential. Thick layers of consolidated or unconsolidated sediments usually mask geophysical anomalies making it difficult to interpret. Airborne magnetic and radiometric maps of Agbabu area reveal magnetic intensity and good contrast between geological structures and their host lithologies providing information useful for structural delineation. The interpreted radiometric data reveal geochemical information on uranium (U), thorium (Th) and potassium (K) and give vital clues about bedrock lithology in that area. The integration of airborne geophysical data (magnetic and radiometric) within the study area helps to delineate zones with capacity to store bitumen, variations of bedrock composition and overall basement characteristics. Also, the datasets were helpful in the identification of aerial extent of bitumen in the study area. The bitumen deposits was clearly mapped. The contact between the metavolcanic and the metasediment is characterized by lateral change in lithological properties. This information inferred from the aeromagnetic maps show the detailed assessment of the contact zone having very low magnetic anomaly



trending NE-SW direction. The maps also show the basement ridge and lithological boundary constraining further migrating of bitumen deposit to other regions.

### References

- [1]. Adegoke O. S. and Omatsola M. E. (1981). Tectonic Evolution and Cretaceous Stratigraphy of the Dahomey Basin. *J. Min. Geol.* 18 (1): 130-137.
- [2]. Boadi B., Wemegah D. D., and Preko K. (2013). Geological and Structural Interpretation of the Konongo Area of the Ashanti Gold Belt of Ghana from Aeromagnetic and Radiometric data. *International Research Journal of Geology and Mining (IRJGM)* (2276-6618), 3(3), pp. 124-135.
- [3]. Clark D. A. (1997). Magnetic properties of rocks and minerals. *AGSO Journal of Australian Geology and Geophysics*, 17(2): 12 – 22.
- [4]. Debeglia N. and Corpel J. (1997). Automatic 3-D Interpretation of Potential Field Data Using Analytic Signal Derivatives. *Geophysics*, 62: 87-96.
- [5]. Geosoft Inc. (1995). OASIS Airborne Radiometric Processing System Version 1.0 User's Guide, Geosoft Incorporated, Toronto.
- [6]. Gunn P. J., Minty B. R. S., and Milligan P. (1997). The airborne gamma-ray spectrometric response over arid Australian terrains. *Exploration*, 97: pp. 733–740.
- [7]. Jones H. A., Hockey R. D. (1964). The Geology of Part of South-western Nigeria". *Geol. Surv. Nigeria Bull.* 31: 87.
- [8]. Keating P. B., (1995). A simple Technique to Identify Magnetic Anomalies Due to Kimberlite Pipes. *Exploration and Mining Geology*, 4: 121-125.
- [9]. Obiora D. N., Mirianrita N. O. and Okwoli E. (2015). A case study of aeromagnetic data interpretation of Nsukka area, Enugu State, Nigeria, for hydrocarbon exploration.
- [10]. Ostrovskiy E. A. (1975). Antagonism of radioactive elements in wellrock alteration fields and its use in aero-gamma spectrometric prospecting. *International Geological Review*, 17: pp. 461–8.
- [11]. Shives R., Charbonneau B., and Ford K. (2000). The detection of potassic alteration by gamma-ray spectrometry-recognition of alteration related to mineralization. *Geophysics-Wisconsin. The Tulsa-Society of Exploration Geophysicists*, 65(6): 2001–2011.
- [12]. Oruc B., and Selim H. (2011). Interpretation of magnetic data in the Sinop area of Mid Black Sea, Turkey, using tilt derivative, Euler deconvolution, and discrete wavelet transform. *Journal of Applied Geophysics*, 74: 194–204.
- [13]. Wemegah D. D., Menyeh A., and Danuor S. K. (2015). Magnetic Susceptibility Characterization of mineralized and non-mineralized rocks of the Subenso Concession of Newmont Ghana Gold Limited. In *Ghana Science Association Biennial Conference, UCC*.
- [14]. Salem A., Williams S., Fairhead J., Ravat D., and Smith R. (2007). Tilt-depth method: a simple depth estimation method using first-order magnetic derivatives. *The Leading Edge*, 26: 1502-1505.
- [15]. Shanks Pat W. C. (2010). Hydrothermal Alteration. Volcanogenic massive sulfide occurrence Model (Scientific Investigation Report).
- [16]. Shives R., Charbonneau B., and Ford K. (2000). The detection of potassic alteration by gamma-ray spectrometry-recognition of alteration related to mineralization. *Geophysics-Wisconsin. The Tulsa-Society of Exploration Geophysicists*, 65(6): pp. 2001–2011.
- [17]. Silva A. M., Pires A. C. B., McCafferty A., Moraes R. A. V., and Xia H. (2003). Application of airborne geophysical data to mineral exploration in the uneven exposed terrains of the Rio Das Velhas greenstone belt. *Revista Brasileira de Geociências*, 33(2):17–28.
- [18]. Reid A. B., Allsop J. M., Granser A., Millett A. J., Somerton I. W., (1990) Magnetic interpretation in three dimension using Euler deconvolution. *Geophysics*. 55, 80–91.

IOSR Journal of Applied Geology and Geophysics (IOSR-JAGG) is UGC approved Journal with Sl. No. 5021, Journal no. 49115.

Ogungbemi. " Geophysical Interpretation of Geological Features Constraining Bitumen Deposit In Agbabu, Southwestern Nigeria. "IOSR Journal of Applied Geology and Geophysics (IOSR-JAGG) 7.4 (2019): 36-44.